

# Dynamical scaling and isotope effect in temporal evolution of mesoscopic structure during hydration of cement

S. Mazumder,<sup>1,\*</sup> D. Sen,<sup>1</sup> R. Loidl,<sup>2</sup> and H. Rauch<sup>2</sup><sup>1</sup>*Solid State Physics Division, Bhabha Atomic Research Centre, Mumbai 400 085, India*<sup>2</sup>*Atominstytut der Österreichischen Universitäten, A-1020 Wien, Austria, and Institut Laue-Langevin, BP 156, 38042 Grenoble Cedex 9, France*

(Received 6 May 2011; revised manuscript received 6 September 2011; published 12 October 2011)

The evolution of mesoscopic structure for cement-water mixtures turning into colloidal gels remains far from being understood. Recent neutron scattering investigations [Phys. Rev. Lett. **93**, 255704 (2004); Phys. Rev. B **72**, 224208 (2005); Phys. Rev. B **82**, 064203 (2010)] reveal the role of the hydrogen bond in the temporal evolution of the mesoscopic structure during hydration of cement, which is the most consumed synthetic material. The present neutron scattering investigation on hydration of cement with a mixture of light and heavy water points to incomprehensibility of the temporal evolution of the mesoscopic structure in terms of earlier observations on hydration with pure light or heavy water. Unlike the case of hydration with light water, disagreement has been observed with the hypothesis of dynamical scaling for hydration of cement with a mixture of the two types of water. The dynamics of evolution of the mesoscopic structure has been observed to be nonlinear in regard to the composition of hydration medium.

DOI: [10.1103/PhysRevB.84.134302](https://doi.org/10.1103/PhysRevB.84.134302)

PACS number(s): 64.75.-g, 61.43.Hv, 61.50.Ks

## I. INTRODUCTION

Investigations on dynamics of new phase formation involve mapping of the time-dependent scattering function  $S(\mathbf{q}, t)$ , where  $t$  stands for time and  $q$  is the modulus of the scattering vector  $\mathbf{q}$ . Because of the isotropic nature of the system at mesoscopic scales,  $S(\mathbf{q}, t)$  is only a function of  $q$ . At late stages, the dynamics of new phase formation is a highly nonlinear process far from equilibrium. The new phase-forming systems exhibit a self-similar growth pattern with dilation symmetry, with a time-dependent scale and scaling phenomenon.<sup>1</sup> The scaling hypothesis assumes the existence of a single characteristic length scale  $L(t)$ , such that the domain sizes and their spatial correlation are time invariant, as depicted in Fig. 1, when the lengths are scaled by  $L(t)$ . Exhibition of dynamical scaling implies that domains, very large in number for a conceivable macroscopic system, are in communication with each other such that they are scaled by the same characteristic length  $L(t)$ . For a  $d$ -dimensional Euclidean system, simple scaling ansatz,<sup>1</sup>  $S(\mathbf{q}, t) = L(t)^d \tilde{F}[qL(t)]$ , holds good at a later time, where  $\tilde{F}(x)$  is the scaled scattering function.

Reaction of cement with water is exothermic in nature, with production of crystalline  $\text{Ca}(\text{OH})_2$  and a noncrystalline colloidal gel-like calcium silicate hydrate (C-S-H). The progress of the reaction, as manifested by the heat evolution rate, has been observed<sup>2-4</sup> to be oscillatory in nature, indicating different stages of hydration. It is to be noted that some structural changes in the system can also cause liberation or absorption of heat. However, compressive strength of the cement-water mixture increases<sup>5</sup> monotonically with time, albeit with varying slopes. The development of compressive strength is also indicative of the existence of one or more processes (e.g., chemical, structural, or a combination of both) in the system. It is desirable to know the contribution and relative significance of each of these processes toward development of compressive strength. It is only expected that temporal evolution of compressive strength bears some

relation, hitherto unknown, with temporal change of heat liberation rate.

Progress of the reaction, as monitored by temporal evolution of  $S(\mathbf{q}, t)$  in recent neutron scattering measurements,<sup>6-9</sup> has been observed to be nonlinear in nature and strongly dependent on the scale of observation and on the medium of hydration (light or heavy water). Although investigation<sup>10</sup> of cement is more than a century old, the temporal evolution of mesoscopic structure, as revealed by these measurements, does not exhibit a well-defined correlation with the existing data on time-dependent change in either compressive strength or heat liberation rate.

The mesoscopic structure of C-S-H gel determines the desirable properties of hardened cement. To elucidate the microscopic structure of the C-S-H gel, many models<sup>11-16</sup> have been proposed. The investigations,<sup>6-9,17,18</sup> based on small-angle neutron scattering (SANS), on continuous temporal evolution of mesoscopic structure during hydration of cement are only recent. The small-angle scattering (SAS) technique can elucidate mesoscopic structure at length scales of  $10^2$ – $10^4$  Å and is an ideal probe for time-resolved structural investigation on C-S-H gel. Both neutrons and X-rays are used as probing radiation for SAS investigations. Neutrons, owing to their considerably higher penetration power, probe larger sample volumes. Neutrons are not invasive because they leave the structure of the sample unaltered and scatter very effectively from hydrogen-bearing materials, such as those found in hydrated cements.

Small-angle X-ray<sup>19</sup> scattering (SAXS) and SANS studies have demonstrated the fractal morphology of C-S-H gel. Furthermore, SAXS investigations have demonstrated<sup>19-21</sup> that C-S-H gel undergoes transition from a ramified to a relatively more compact structure. A structure is said to be more ramified<sup>22</sup> at a particular point if more number of bonds are to be eliminated to isolate an arbitrarily large bounded substructure surrounding that point. All other structural parameters remaining the same, a more ramified structure will have

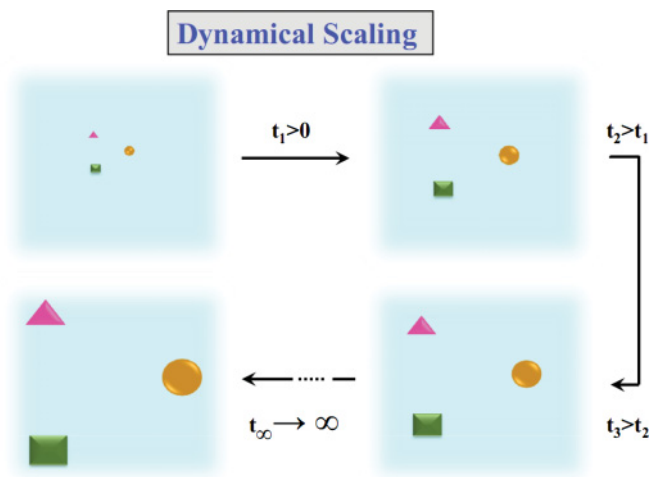


FIG. 1. (Color online) A schematic representation of dynamical scaling. Individual inhomogeneities are scaled up by the same time dependent scale factor  $L(t)$ , implying some communication mechanism between the individual inhomogeneities.

less mass and hence a more open, vis-à-vis one with a lesser ramified structure. For a ramified mass fractal structure with fractal dimension  $D_m$  embedded in a three-dimensional space, the value of  $D_m$  lies in the range  $1 < D_m < 3$ . For a ramified rod and disk, the value of  $D_m$  lie in the range  $0 < D_m < 1$  and  $1 < D_m < 2$ , respectively. The smaller the value of  $D_m$ , the more ramified is the object.

Examinations, involving continuous monitoring of the temporal evolution of mesoscopic structure during hydration of cement with light water ( $H_2O$ ) and heavy water ( $D_2O$ ), have been reported<sup>6–9</sup> only recently. It has been observed<sup>6–9</sup> that the kinetics of hydration of silicates and sulfates with light and heavy water are of nonlinear nature, even at the initial time. Although the formation of hydration products is synchronous for hydration with  $H_2O$ , the process is nonsynchronous for hydration with  $D_2O$ . Time-resolved experiments,<sup>6,7</sup> with hydration time not exceeding 5 hours, investigating the temporal evolution of morphological features at length scales of  $10^3–10^4$  Å, of hydrated gel C-S-H and C-S-D, have indicated that for hydration of cement with  $H_2O$ , topographical mesoscopic structure could not be described in terms of a classical porous medium with a well-defined specific inner surface. The mesoscopic structure, at length scales of  $10^3–10^4$  Å, is initially that of a mass fractal.

In the case of hydration of silicates with light water, the hydrating mass exhibits<sup>6,7</sup> a mass fractal nature, at length scales of  $10^3–10^4$  Å, for the initial few (2–3) hours of hydration, the mass fractal dimension increasing with time and reaching a plateau after about 150 min, with the maximum attained value less than 3. The second phase grows with time initially. Subsequently, the domain size of the second phase saturates. Temporal evolution of the square of the linear dimension of the inhomogeneity mimics<sup>6,7</sup> the trend of the temporal evolution of the fractal dimension. At large time limits, the temporally evolving system exhibits a self-similar growth pattern with dilation symmetry and with the scaling phenomenon.<sup>1</sup>

In view of aforementioned observations,<sup>6–9</sup> it has been concluded that for hydration of cement with  $H_2O$ , water-rich mass fractal C-S-H sol and crystalline  $Ca(OH)_2$  are formed initially. The  $Ca(OH)_2$  phase is a minor phase, and the fractal structure, as observed in scattering measurements, pertains to major C-S-H phases because pores cannot exhibit mass fractal nature. Both the fractal dimension and linear dimension of the mass fractal C-S-H phase grow with time. The initial increase of the mass fractal dimension with time reflects the transition from a ramified and porous structure to a relatively more compact homogeneous solid matrix. Because the system exhibits dynamical scaling phenomena, the ratio of the linear sizes of  $Ca(OH)_2$  crystallite and the C-S-H phase must be constant, indicating the growth (Fig. 1) of linear size in both phases by the same characteristic length with time, implying the synchronous formation of  $Ca(OH)_2$  and C-S-H in this period of hydration. At length scales of  $10^2–10^3$  Å, morphological change<sup>9</sup> of the mesoscopic structure is much more monotonic in nature.

The hydration of silicates with light or heavy water is expected to be similar, except for their kinetics. Because of higher molecular mass, diffusion is expected to be more sluggish for heavy water. Furthermore, it is known that the hydrogen bond with deuterium is slightly stronger than that involving ordinary hydrogen<sup>23</sup> because of higher reduced mass and, hence, lower energy at the same level, including the zero-point energy of the bond of diatomic molecules involving deuterium vis-à-vis that involving hydrogen, which is also responsible for the shorter bond length in O-D vis-à-vis that in O-H. With a lower energy, more energy is required to overcome the activation barrier for bond cleavage or dissociation. In fact, with heavier elements like oxygen, calcium, or silicon, the frequency or energy of a bond involving D is approximately  $1/\sqrt{2}$  times that of the corresponding bond involving H. Hence, it is expected that hydration with  $D_2O$  will be slower compared with that of  $H_2O$  because of higher activation energy. Moreover, hydration products involving deuterium will be more stable than those involving hydrogen. The lifetime of the hydrogen bond involving D is longer vis-à-vis that involving H because the vibrational motions perpendicular to the bond direction have smaller amplitudes for D than that for H because of the difference in isotopic mass.

Some contrasting behavior has been observed<sup>6,7,9</sup> in the case of hydration of silicates with heavy water. The domain size of the density fluctuations grows in the beginning for a while and subsequently shrinks with time. Mesoscopic structure, at length scales of  $10^3–10^4$  Å, undergoes transition from mass fractal to surface fractal, and finally again to mass fractal. No agreement has been observed<sup>6,7</sup> with the dynamical scaling hypothesis for all possible measures of the characteristic length. At length scales of  $10^2–10^3$  Å, morphological change<sup>9</sup> in the mesoscopic structure is much wider. It is a conjecture that different rates of diffusion of light and heavy water in forming a gel structure in silicates lead to the formation of different structural networks with different scattering contrasts.

The above observations call for examining the temporal evolution of the mesoscopic structure encountered during hydration of cement with a mixture of  $H_2O$  and  $D_2O$ . Investigations on nonlinearity and its modulations when the hydration medium is mixed is a subject of importance. This is

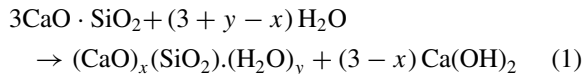
also to understand better the role of the hydrogen bond in the hydration behavior of cement.

## II. EXPERIMENT

Water mixtures, comprising light water ( $\text{H}_2\text{O}$ ) and heavy water ( $\text{D}_2\text{O}$ ) at molar ratios of 3:1, 1:1, and 1:3, were prepared initially for hydration of cement. Pure powder specimens of tricalcium silicate ( $\text{C}_3\text{S}$ ) were mixed with water mixtures at varying water-to-cement ( $w/c$ ) mass ratios, ranging from 0.3 to 0.5 to obtain a wet mass. C-S-H gel is known<sup>6,7,9</sup> to have fractal mesoscopic structure at length scales of  $10^2$ – $10^3$  Å. A preliminary measurement with medium-resolution SANS<sup>24</sup> indicated that hydrated cement has a fractal microstructure at length scales of 1–100 nm. It also indicated the possibility of the existence of inhomogeneities larger than 100 nm, so SANS measurements were carried out with ultra-SANS instrument<sup>25</sup> S18 at a 58-MW high flux reactor at Institut Laue-Langevin (Grenoble, France). The wavelength ( $\lambda$ ) used was 1.87 Å. The scattered intensities were recorded as a function of  $q (= 4\pi(\sin \theta)/\lambda, 2\theta$  being the scattering angle). The scattering data were corrected for background and primary beam geometry. For correction of background, scattering measurements have been carried out at about  $q = 10^{-2}$  (Å)<sup>-1</sup>. At the outset, it was inferred that hydrating specimens are isotropic in nature and so is the scattering function<sup>26</sup>  $S(\mathbf{q}, t)$ .

## III. DATA INTERPRETATION AND DISCUSSION

The present work reports the mesoscopic structural investigations on real-time hydration of cement. Widely used Portland cement<sup>5</sup> is a composite material consisting of fine crystalline grains of tricalcium silicate,  $3\text{CaO} \cdot \text{SiO}_2$  (abbreviated  $\text{C}_3\text{S}$ ; approximate mass percentage range 60%–80%), along with minor constituents like dicalcium silicate, tricalcium aluminate, tetracalcium iron aluminate, and so on. As the major constituent of Portland cement,  $\text{C}_3\text{S}$  can be used as a model for hydration of cement. The hydration reaction of  $\text{C}_3\text{S}$  can be written as



where  $x$  and  $y$  vary,  $x$  is bounded by  $0 \leq x \leq 3$  and  $y$  measures the partitioning of reacted  $\text{H}_2\text{O}$  between  $(\text{CaO})_x(\text{SiO}_2)_y(\text{H}_2\text{O})_y$  and  $\text{Ca}(\text{OH})_2$  phases. The variable  $y$  is bounded on one side (i.e.,  $y \geq 0$ ), and  $y = 0$  indicates consumption of the entire reacted  $\text{H}_2\text{O}$  in the formation of  $\text{Ca}(\text{OH})_2$ .  $x = 3$  indicates hydration of  $\text{C}_3\text{S}$  without formation of  $\text{Ca}(\text{OH})_2$ . Recently it has been established that  $x$  is time dependent and the functional form of  $x(t)$  is dependent on the hydration medium ( $\text{H}_2\text{O}$  or  $\text{D}_2\text{O}$ ).<sup>9</sup> pH dependence of the kinetics of reaction is a plausible reason for the time dependence of  $x(t)$ . The product  $(\text{CaO})_x(\text{SiO}_2)_y \cdot (\text{H}_2\text{O})_y$  (abbreviated C-S-H, wherein hyphens indicate variable stoichiometry) is calcium silicate hydrate—a colloidal gel-like polymeric material at the late stage of hydration. Tricalcium silicate ( $\text{C}_3\text{S}$ ) and  $\text{Ca}(\text{OH})_2$  are both crystalline in nature. Because reaction (1) involves cleavage of H-OH bond and formation of new bonds, it should be termed hydrolysis rather than hydration; however, we will continue to use the term hydration for reaction (1).

Figure 2 depicts the time evolution of the scattering function  $S(\mathbf{q}, t)$  with an absolute scale for a water mixture hydrating  $\text{C}_3\text{S}$  with  $w/c = 0.3$  and  $w/c = 0.5$ , respectively. Different curves in each frame depict the variation of  $S(\mathbf{q}, t)$  with  $q$  for different recorded times. The inset of the figure depicts the temporal variation of  $S(\mathbf{q}, t)$  at an arbitrary scale for three specific values of  $q$ , as mentioned therein. For a system with a polydisperse population of inhomogeneities and degree of polydispersity  $m$ ,  $S(\mathbf{q}, t)$  is given by

$$S(\mathbf{q}, t) = \sum_{i=1}^m \tau_i(t) V_i^2(t) \rho_i^2(t) P_i(q) = \sum_{i=1}^m \tau_i(t) \zeta_i^2(t) P_i(q)$$

where the subscripted quantities  $\tau_i$ ,  $V_i$ ,  $\rho_i$ ,  $P_i(q)$ , and  $\zeta_i (= V_i \rho_i)$  are respectively the number density, volume, scattering length density, normalized scattering form factor, and total scattering length integrated over volume of the  $i$ th type of inhomogeneity. Normalized scattering form factor  $P_i(q) \rightarrow 1$  as  $q \rightarrow 0$ . For a spherical inhomogeneity of radius  $r_0$ ,

$$P(q) = 9 \frac{[\sin(qr_0) - qr_0 \cos(qr_0)]^2}{(qr_0)^6}$$

An inhomogeneity is defined by the uniform scattering length density over its volume. It is important to note that  $S(\mathbf{q}, t)$  has parabolic dependence on  $\zeta$ .

The oscillatory nature of temporal evolution of  $S(\mathbf{q}, t)$  for specified  $q$  values is indicative of the fact that there are competing factors<sup>9</sup> for temporal evolution of  $S(\mathbf{q}, t)$ —some causing decay and others causing growth of  $S(\mathbf{q}, t)$  with time resulting in non-monotonic temporal evolution of  $S(\mathbf{q}, t)$ . To appreciate the oscillatory nature of  $S(\mathbf{q}, t)$  as depicted in inset of Fig. 2, some model calculations (Model Calculations in Appendix) for hydration of cement have been considered. Some more general cases depicting the oscillatory variation of  $S(\mathbf{q}, t)$  with  $t$  for  $q = 0$  has already been dealt with earlier.<sup>9</sup>

Insets of Fig. 3 indicate that with increasing hydration time, the curvature of the scattering profiles in the vicinity of  $q \rightarrow 0$ , varies non-linearly indicating the nonlinearity in the growth of pores. The curvature  $\kappa(t)$  of normalized  $S(\mathbf{q}, t)$  at  $q$  is given by

$$\kappa(t) = \frac{|d^2[S(\mathbf{q}, t)/S(0, t)]/dq^2|}{(1 + \{d[S(\mathbf{q}, t)/S(0, t)]/dq\}^2)^{3/2}}$$

For a monodisperse population of inhomogeneity, the linear dimension of the inhomogeneity is proportional<sup>27</sup> to  $\sqrt{\kappa(t)}$ . The curvature<sup>27</sup>  $\kappa(t)$  in the vicinity of  $q \rightarrow 0$  of a scattering profile  $S(\mathbf{q}, t)$  is related to

$$G(t) = -d\{\ln[S(\mathbf{q}, t)/S(0, t)]\}/dq^2$$

where  $G(t)$  is the negative gradient of the Guinier plot of the normalized scattering profile. For a single scattering profile from a monodisperse population of spheres of radius  $R$ , near  $q \rightarrow 0$ ,  $\kappa = 2R^2/5$ , whereas  $G = R^2/5$ . In subsequent discussions,  $\kappa$  is defined for  $q \rightarrow 0$  only, throughout, if not mentioned otherwise. For a polydisperse population of spherical scatterers with number density  $n(R)$  for scatterers of radius  $R$ , having the same scattering length density difference,  $\kappa = 2\langle R^8 \rangle / 5\langle R^6 \rangle$ , where  $\langle R^n \rangle$  is the  $n$ th moment of

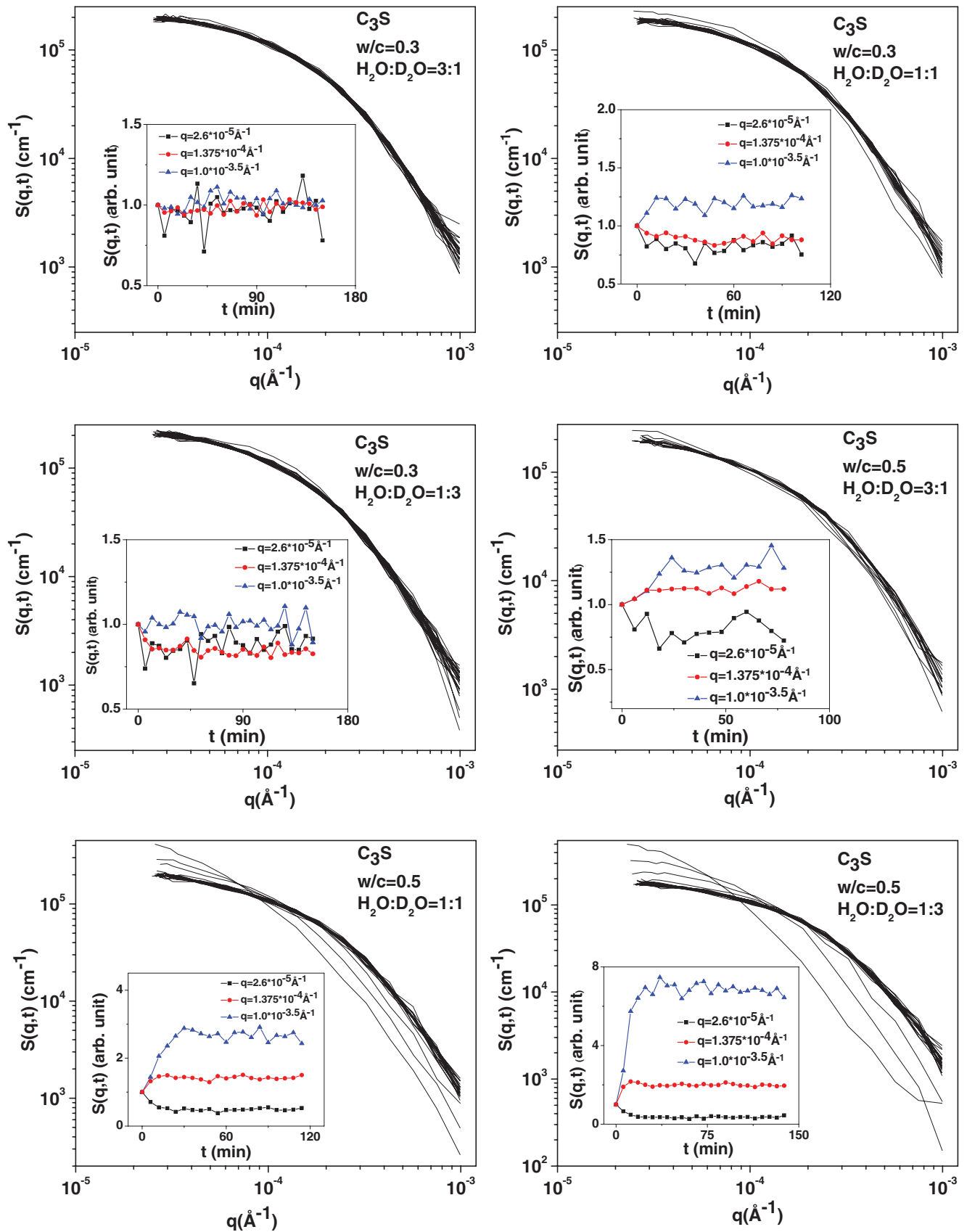


FIG. 2. (Color online) Time evolution of scattering function  $S(q, t)$  for a water mixture hydrating  $C_3S$  with a water-to-cement mass ratio ( $w/c$ ) = 0.3 and 0.5, respectively. The inset shows the time evolution of  $S(q, t)$  at some specified values of  $q$  as specified therein. Statistical error bars are smaller than the respective symbol sizes.

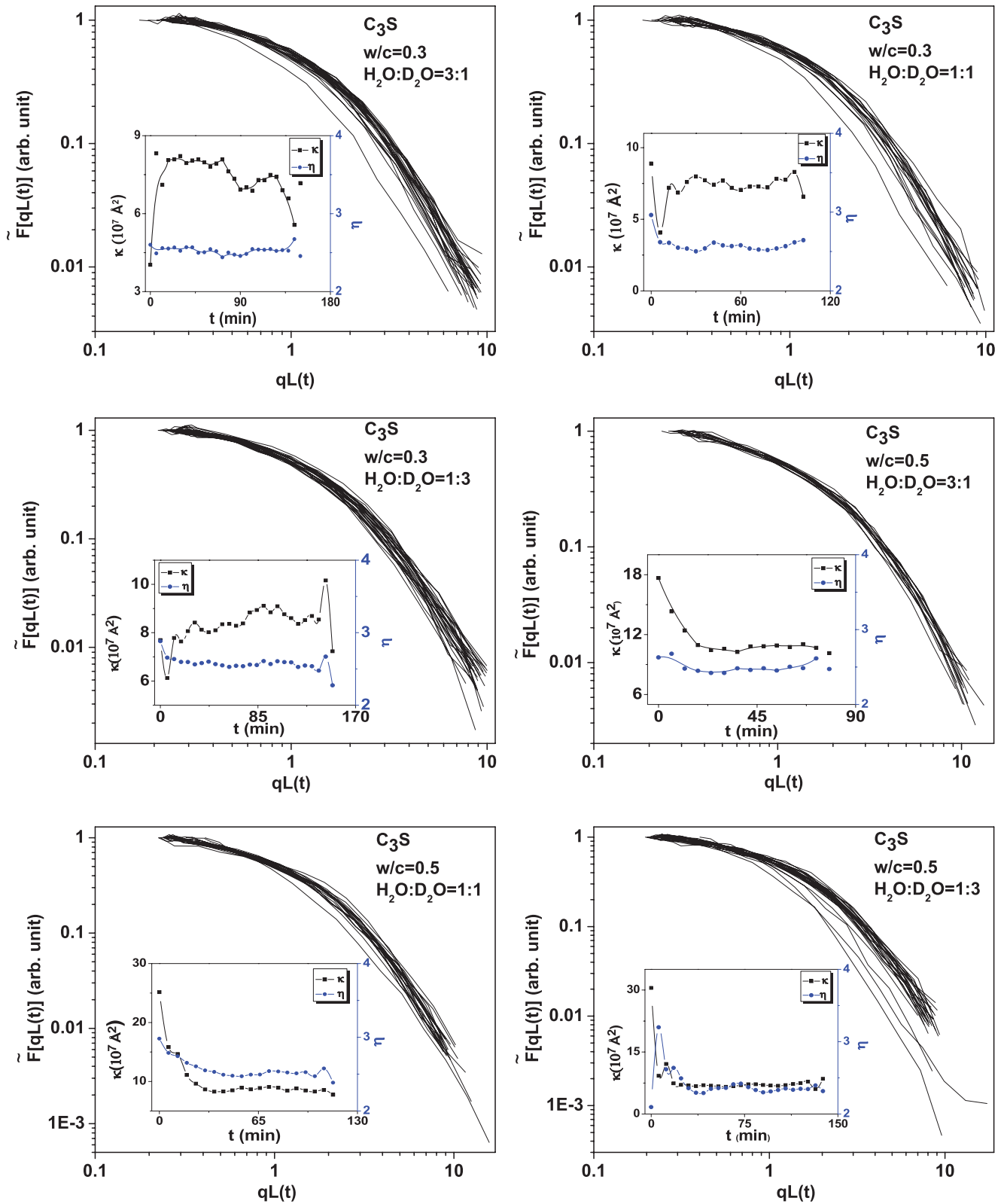


FIG. 3. (Color online) Scaled scattering function  $\tilde{F}[qL(t)]$  for a water mixture hydrating  $C_3S$  with a water-to-cement mass ratio ( $w/c$ ) = 0.3 and 0.5, respectively. The inset shows the time evolution of  $\kappa(t)$  and  $\eta(t)$ , associated with power law scattering. Statistical error bars are smaller than the respective symbol sizes. The solid lines are only guides for the eye.

the distribution  $n(R)$ . Curvature<sup>27</sup> and radius of curvature are reciprocal to each other.

The insets of Fig. 3 also depict the temporal evolution of  $\kappa(t)$  for a water mixture hydrating  $C_3S$  with  $w/c = 0.3$  and  $w/c = 0.5$ , respectively. For all hydrating specimens with  $w/c = 0.3$ ,  $\kappa(t)$  vs.  $t$  has an oscillatory nature irrespective of mixture composition. For hydrating  $C_3S$  with water mixtures having molar ratios  $H_2O:D_2O = 3:1$  and  $1:3$ , oscillations depict decreasing and increasing trends, respectively, of  $\kappa(t)$  vs.  $t$ . However, for hydrating specimens with water mixture molar ratio  $H_2O:D_2O = 1:1$ , oscillations without any distinct trend are observed.

For a hydrating specimen with  $w/c = 0.5$ , irrespective of mixture composition,  $\kappa(t)$  sharply decreases with time and reaches a plateau. These results are strikingly different from those observed<sup>6,7</sup> for hydration of silicates with pure light water or heavy water. It is pertinent to recall<sup>6,7</sup> that for hydration of silicates with light water,  $\kappa(t)$  vs.  $t$  has similar generic variation irrespective of value of  $w/c$ , as is the case for hydration of silicates with heavy water. For hydration of silicates with light water,  $\kappa(t)$  increases with time initially and saturates subsequently. For hydration of silicates with heavy water,  $\kappa(t)$  increases<sup>6,7</sup> with time initially, reaches a peak, and finally decreases as time increases.

As recently observed<sup>9</sup> when mixing silicates with water, water-rich C-S-H colloidal sol particles, a colloidal phase of solid dispersed in continuous liquid phase, are formed initially. Depending on the relative strength of thermal energy and the energy barrier between particles, the aggregation of colloidal particles occurs according to well-defined<sup>28</sup> regimes of diffusion-limited cluster aggregation (DLCA) and reaction-limited cluster aggregation (RLCA). DLCA occurs when thermal energy is relatively higher than the barrier energy so that every collision, limited only by the rate of diffusion of the colliding particles, results in colliding particles sticking together, leading to rapid aggregation and cluster mass growing linearly with time. RLCA occurs when thermal energy is relatively lower or comparable to the barrier energy, so that out of several collisions, one collision results in colliding particles sticking together, leading to slower aggregation and cluster mass growing exponentially with time. In the latter case, aggregation is limited by the probability of overcoming the energy barrier—hence, the name reaction-limited cluster aggregation. In RLCA, a cluster with larger mass has more potential bonding sites and grows faster than the smaller clusters.

For hydration of silicates with pure light water and heavy water, initial increase<sup>6,7</sup> of  $\kappa(t)$  with time is not exponential and can be linearly approximated, indicating the role of the diffusion-limited aggregation process in growth of domains. The observed deviation from the DLCA regime in the later stage, and also somewhat in the initial stage, indicates the role of some other effect, like hydrogen bonding. Because a hydrogen bond involving deuterium is somewhat stronger than one with hydrogen, it leads to consolidation of the C-S-D mass fractal colloidal particle into a mass with Euclidean core and with surface fractal morphology. For hydration of silicates with water mixture, the observed temporal variation of  $\kappa(t)$  with  $t$  only indicates a plausible role of hydrogen bonding.

The insets of Fig. 3 also depict time evolution of the Porod exponent  $\eta(t)$ , as estimated from  $\ln[S(\mathbf{q}, t)]$  vs.  $\ln(q)$  for  $0.00025 < q < 0.001 \text{ \AA}^{-1}$ , for a water mixture hydrating  $C_3S$  with  $w/c = 0.3$  and  $w/c = 0.5$ , respectively. The Porod exponent for all hydrating specimens lies in the range of 2–3, indicating the mass fractal nature of the hydrating paste. For objects whose volume or mass is fractal (cluster aggregates),  $S(\mathbf{q}, t)$  asymptotically approaches a form  $S(\mathbf{q}, t) \sim q^{-\eta(t)}$ , where the exponent  $\eta$  reflects<sup>29</sup> directly the mass fractal dimension  $D_m$ . For a mass fractal object embedded in a three-dimensional space,  $\eta = D_m$  with  $1 < \eta, D_m < 3$ . For a water mixture hydrating specimen, irrespective of mixture composition,  $\eta(t)$  initially decreases marginally with time and reaches a plateau with minor oscillations without any distinct trend. The generic variations of  $\kappa(t)$  vs.  $t$  and  $\eta(t)$  vs.  $t$  differ widely. These results are strikingly different from those observed<sup>6,7</sup> for hydration of silicates with pure light water or heavy water. It is noteworthy<sup>6,7</sup> that for hydration of silicates with light water,  $\eta(t)$  vs.  $t$  has generic variation similar to  $\kappa(t)$  vs.  $t$ , irrespective of the  $w/c$  value, and so is the case for hydration of silicates with heavy water. For hydration of silicates with light water,  $\eta(t)$  increases<sup>6,7</sup> with time initially and saturates subsequently. For hydration of silicates with heavy water,  $\eta(t)$  increases<sup>6,7</sup> with time initially, reaches a peak, and finally decreases as time increases.

In accordance with the linear theory<sup>30</sup> of new phase formation, the temporal variation of scattering function  $S(\mathbf{q}, t)$  is given by:

$$S(\mathbf{q}, t) = S(\mathbf{q}, 0) \exp[2t\alpha(q)]$$

where  $\alpha(q)$  is the time-independent proportionality constant.

It has been observed that  $\alpha(q)$  does not behave in a time-independent fashion for all hydrating specimens discussed in the present work, even at the initial stage of measurement, indicating the inadequacy of linear theory to comprehend the observations of the present set of measurements.

To examine the scattering function kinetics in the light of dynamical scaling phenomenon, based on nonlinear theories,<sup>1</sup> of new phase formation, the normalized scaling function  $\tilde{F}[qL(t)] = S(\mathbf{q}, t) [L(t)]^{-D_m} / \sum q^{D_m} S(\mathbf{q}, t) \delta q$  has been calculated where  $L(t) = \sqrt{\kappa(t)}$  and  $\delta q$  is the experimental  $q$  increment.

It is important to note that for a mass fractal object, surface area also scales<sup>31</sup> as  $r^{D_m}$  for a spherical surface of radius  $r$ . The variations of  $\tilde{F}[qL(t)]$  with  $qL(t)$  for a water mixture hydrating  $C_3S$  with  $w/c = 0.3$  and  $w/c = 0.5$  are shown in Fig. 3. Different curves in each frame depict the variation of  $\tilde{F}[qL(t)]$  with  $qL(t)$  for different recorded times. It is evident from the figure that the scaling functions are not strictly time independent, indicating poor agreement with the scaling hypothesis. These results are in sharp contrast to those observed<sup>6,7</sup> in the case of light water hydrating specimens of silicates. In the case of hydrating silicates, good agreement with the scaling hypothesis has been observed for a wide range of  $w/c$  values. It has also been observed that the scaling phenomenon is also not operative for all water mixtures hydrating  $C_3S$  specimens under investigation for  $L(t) = [q_1(t)]^{-1}$ , where  $q_1(t)$  is the first moment of the scattering function  $S(\mathbf{q}, t)$ .

It remains to be understood why scaling is observed in hydration of silicates, tricalcium silicate, and dicalcium silicate with pure H<sub>2</sub>O but not with either pure D<sub>2</sub>O or with a mixture of H<sub>2</sub>O and D<sub>2</sub>O. As has been observed,<sup>9</sup> when silicates are mixed with H<sub>2</sub>O, a water-rich C-S-H colloidal sol is formed initially. For this very reason, the temporal evolution of the mesoscopic structure of a C-S-H gel will not be influenced by the microscopic structure of the silicate or its particle size distribution, although initial dissolution rate could depend on microscopic structure and particle size distribution. The morphology of the H<sub>2</sub>O hydrating colloidal particle is a mass fractal, with fractal dimension increasing with time initially and reaching a plateau.

For hydration with D<sub>2</sub>O, the sol changes<sup>6,7</sup> topographically with time, unlike the case of hydration with H<sub>2</sub>O. In the beginning, the sol is ramified throughout the volume, but the degree of ramification decreases with time. Subsequently, the mass transforms into objects with uniform internal density of unramified core with ramified surface showing self-similarity. Later, the ramified surface grows into ramified volume during hydration—the degree of ramification increasing with time. This topographical change of the hydrating mass as a function of time is one of the plausible reasons why scaling is not observed in the case of hydration of silicates with D<sub>2</sub>O. Furthermore, the formation rates of C-S-D and Ca(OD)<sub>2</sub> vary differently with time for hydration with D<sub>2</sub>O. As a consequence, the ratio of linear sizes of Ca(OD)<sub>2</sub> crystallite and the C-S-D phase vary with time. This is another reason why scaling is not observed for hydration with D<sub>2</sub>O. However, for hydration with a water mixture, the sol does not change topographically with time. It remains a mass fractal throughout with marginal variation of fractal dimension. Temporally, varying formation rates leading to different growth kinetics of radii of C-S-H, C-S-D, Ca(OH)<sub>2</sub>, and Ca(OD)<sub>2</sub> provide a plausible reason why scaling is not observed in the case of hydration with a water mixture. It is noteworthy that for both light and heavy water hydration of sulfates, time evolution of the scattering functions do not exhibit scaling phenomena<sup>1</sup> for a characteristic length with any possible measure, although there is no topographical change of the hydrating mass as a function of time. The hydrating mass remains a mass fractal throughout.

IV. CONCLUSIONS

The role of the hydrogen bond is crucial to understand how cement, a crystalline powder, on mixing with liquid water, turns into a monolithic mass structure as one piece with high compressive strength. Using pure light water, pure heavy water, and mixture of the two as the hydration medium is one experimental way to tune the hydrogen bond effect. In the present work, temporal evolution of the mesoscopic structure and hydration kinetics of cement with a mixture of light and heavy water have been investigated. These experimental observations have been compared with the corresponding observations on the hydration of silicates with pure light or heavy water. It has been observed that the dynamics of hydration of cement with a mixture of light and heavy water is incomprehensible in terms of the observed hydration dynamics of cements with pure light or heavy water.

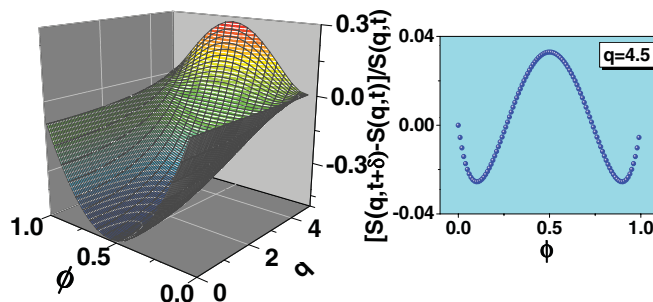


FIG. 4. (Color online) Model calculations depicting fluctuations of  $S(q, t)$  as a function of  $q$  and volume fraction  $\phi$  of a fragmented inhomogeneity for splitting a spherical inhomogeneity into two spherical inhomogeneities, the volume fraction of one split inhomogeneity being  $\phi$ .

Unlike in the case with heavy water, and as in the case with light water, the hydrating mass remains a mass fractal throughout for hydration of silicates with a water mixture—implying no topographical change of the hydrating mass as a function of time. Unlike the case involving light water, the mass fractal dimension does not grow linearly with time initially—implying a nondominant role of the diffusion-limited cluster aggregation mechanism for hydration of silicates with water mixtures. But, as in the case with heavy water and unlike in the case with light water, a scaling phenomenon has not been observed for hydration of silicates with a water mixture—implying nonsynchronous formation of Ca(OH)<sub>2</sub>/Ca(OD)<sub>2</sub> and C-S-H/C-S-D in this period of hydration. Because hydration of cement with light water exhibits dynamical scaling phenomena, the ratio of linear sizes of Ca(OH)<sub>2</sub> crystallite and the C-S-H phase must be constant with time, indicating the synchronous formation of Ca(OH)<sub>2</sub> and C-S-H in this period of hydration. The dynamics of evolution of the mesoscopic structure of hydration of cement

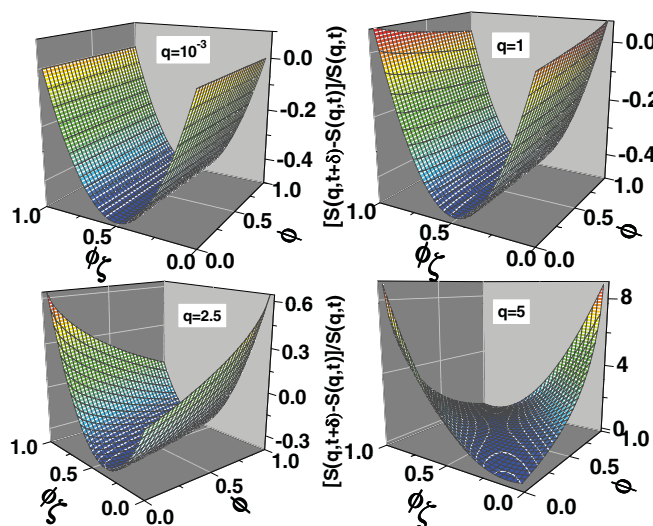


FIG. 5. (Color online) Model calculations depicting fluctuations of  $S(q, t)$  as a function of volume fraction and scattering length fraction at some specified  $q$ -values for splitting of a spherical inhomogeneity into two spherical inhomogeneities. The volume fraction of one split inhomogeneity is  $\phi$  with scattering length fraction  $\phi_\zeta$ .

has been observed to be nonlinear, also with regard to the composition of the hydration medium.

### ACKNOWLEDGEMENT

We are grateful to T. Mazumder and J. Bahadur for their help in making some of the figures.

### APPENDIX

#### Model Calculation

Dealing with the effect of changing coherence characteristic of inhomogeneities on  $S(q, t)$ :

Consider a model system with one inhomogeneity of volume unity with total scattering length  $\zeta$  at time  $t$ . At time  $t + \delta$ , the inhomogeneity transforms into two spherical inhomogeneities with total scattering length  $(\zeta - \alpha)$  and  $\alpha$ , respectively following the conservation of total scattering length and volume. There exists two possibilities in such a situation.

The scattering length densities of the fragmented spherical inhomogeneities remain the same:

Figure 4 depicts the variation of  $\frac{S(q,t+\delta)-S(q,t)}{S(q,t)}$  with  $q$  and volume fraction  $\varphi (= \alpha/\zeta)$  of one fragmented inhomogeneity. Variations are obviously symmetric about  $\varphi = 0.5$ . The oscillatory nature of  $\frac{S(q,t+\delta)-S(q,t)}{S(q,t)}$  is significant at  $q > (\pi/\text{diameter})$  of a sphere of unity volume), and the significance of oscillation increases with an increase of  $\varphi$  (i.e., with increase of the significance of fragmentation).

The scattering length densities of the fragmented spherical inhomogeneities vary:

Figure 5 depicts the variation of  $\frac{S(q,t+\delta)-S(q,t)}{S(q,t)}$  with  $q$  and volume fraction  $\varphi$  of one fragmented inhomogeneity with scattering length fraction  $\varphi_\zeta (= \alpha/\zeta)$ . At  $q \rightarrow 0$ , variations are parabolic and symmetric about  $\varphi_\zeta = 0.5$ . Symmetry breaks with increasing  $q$ . Results will be reversed when two or more inhomogeneities join together to form a coherent mass. A contiguous domain having uniform chemical composition, and hence uniform scattering length density, is termed a coherent mass. Composition modulation leads to incoherence. Scattering centers within a coherent mass scatter coherently.

\*smazu@barc.gov.in.

<sup>1</sup>A. J. Bray, *Adv. Phys.* **43**, 357 (1994), and references therein.

<sup>2</sup>T. C. King, C. M. Dobson, and S. A. Rodger, *J. Mater. Sci. Lett.* **7**, 861 (1988).

<sup>3</sup>G. C. Bye, *Portland Cement: Composition, Production and Properties* (Pergamon Press, Oxford, 1983).

<sup>4</sup>D. P. Bentz, P. V. Coveney, E. J. Garboczi, M. F. Kleyn, and P. E. Stutzman, *Modell. Simul. Mater. Sci. Eng.* **2**, 783 (1994) and [<http://ciks.cbt.nist.gov/garbocz/cell1994/node4.htm>].

<sup>5</sup>H. F. W. Taylor, *The Chemistry of Cements* (Academic Press, London, 1964).

<sup>6</sup>S. Mazumder, D. Sen, A. K. Patra, S. A. Khadilkar, R. M. Cursetji, R. Loidl, M. Baron, and H. Rauch, *Phys. Rev. Lett.* **93**, 255704 (2004).

<sup>7</sup>S. Mazumder, D. Sen, A. K. Patra, S. A. Khadilkar, R. M. Cursetji, R. Loidl, M. Baron, and H. Rauch, *Phys. Rev. B* **72**, 224208 (2005).

<sup>8</sup>S. Mazumder, R. Loidl, and H. Rauch, *Phys. Rev. B* **76**, 064205 (2007).

<sup>9</sup>S. Mazumder, D. Sen, J. Bahadur, J. Klepp, H. Rauch, and J. Teixeira, *Phys. Rev. B* **82**, 064203 (2010).

<sup>10</sup>H. L. Le Chatelier, *Experimental Researches on the Constitution of Hydraulic Mortars* (McGraw, New York, 1905).

<sup>11</sup>Z. Xu and D. Viehland, *Phys. Rev. Lett.* **77**, 952 (1996).

<sup>12</sup>I. G. Richardson and G. W. Groves, *Cement and Concrete Research* **22**, 1001 (1992).

<sup>13</sup>H. F. W. Taylor, *J. Am. Ceram. Soc.* **69**, 464 (1986).

<sup>14</sup>S. A. Greenberg, T. N. Chang, and E. Andersen, *J. Phys. Chem.* **64**, 1151 (1960).

<sup>15</sup>S. A. Greenberg and T. N. Chang, *J. Phys. Chem.* **69**, 182 (1965).

<sup>16</sup>K. Fujii and W. Kondo, *J. Am. Ceram. Soc.* **66**, C-220 (1983).

<sup>17</sup>D. Sen, S. Mazumder, and J. Bahadur, *Phys. Rev. B* **79**, 134207 (2009).

<sup>18</sup>T. Mazumdar, S. Mazumder, and D. Sen, *Phys. Rev. B* **83**, 104302 (2011).

<sup>19</sup>M. Kriechbaum, G. Degovics, P. Laggner, and J. Tritthart, *Adv. Ceram. Res.* **6**, 93 (1994).

<sup>20</sup>A. Heinemann, H. Hermann, K. Wetzig, F. Haussler, H. Baumbach, and M. Kroening, *J. Mater. Sci. Lett.* **18**, 1413 (1999).

<sup>21</sup>M. Kriechbaum, G. Degovics, J. Tritthart, and P. Laggner, *Prog. Colloid Polym. Sci.* **79**, 101 (1989).

<sup>22</sup>A. Gefen, A. Aharony, Y. Shapir, and B. B. Mandelbrot, *J. Phys. A: Math. Gen.* **17**, 435, (1984).

<sup>23</sup>J. J. Katz, *Am. Sci.* **48**, 544 (1960).

<sup>24</sup>S. Mazumder, D. Sen, T. Saravanan, and P. R. Vijayaraghavan, *J. Neutron Res.* **9**, 39 (2001); *Current Science* **81**, 257 (2001).

<sup>25</sup>M. Hainbuchner, M. Villa, G. Kroupa, G. Bruckner, M. Baron, H. Amenitsch, E. Seidl, and H. Rauch, *J. Appl. Cryst.* **33**, 851 (2000).

<sup>26</sup>L. Van Hove, *Phys. Rev.* **95**, 249 (1954).

<sup>27</sup>S. Mazumder, D. Sen, S. K. Roy, M. Hainbuchner, M. Baron, and H. Rauch, *J. Phys. Condens. Matter* **13**, 5089 (2001); N. Pishkunov, *Differential and Integral Calculus, English translation*, (Mir Publishers, Moscow, 1974).

<sup>28</sup>M. Y. Lin, H. M. Lindsay, D. A. Weitz, R. C. Ball, R. Klein, and P. Meakin, *Phys. Rev. A* **41**, 2005 (1990).

<sup>29</sup>T. Freltoft, J. K. Kjems, and S. K. Sinha, *Phys. Rev. B* **33**, 269 (1986); J. Teixeira, in *Experimental Methods for Studying Fractal Aggregates in On Growth and Form*, edited by H. E. Stanley and N. Ostrowsky (Kluwer Academic, Dordrecht, 1986), pp. 145–162.

<sup>30</sup>J. W. Cahn, *Acta Metall.* **9**, 795 (1961).

<sup>31</sup>P. Pfeifer and D. Avnir, *J. Chem. Phys.* **79**, 3558 (1983); **80**, 4573 (1984).